Journal of Sound and Vibration (2000) **234**(3), 471–489
doi:10.1006/jsvi.1999.2871, available online at http://www.idealibrary.com on IDEAL®

REGION-WISE LINEAR FUZZY SLIDING MODE CONTROL OF THE MOTOR–MECHANISM SYSTEMS

RONG-FONG FUNG AND CHIN-CHI SHAW

Department of Mechanical Engineering, Chung Yuan Christian University, Chung Li, Taiwan, 32023, Republic of China. E-mail address: rongfong@cycu.edu.tw

AND

AN-PEI WANG

Department of Civil Engineering, Chung Yuan Christian University, Chung Li, Taiwan, 32023, Republic of China

(*Received* 1 *September* 1999, *and in final form* 23 *December* 1999)

In this paper, the fuzzy sliding mode controller (FSMC) and region-wise linear fuzzy sliding mode controller (RLFSMC) are applied to toggle and quick-return mechanisms, which are driven by a permanent magnet (PM) synchronous servomotor. The FSMC and RLFSMC are robust controllers developed to regulate the slider position of the coupled motor-mechanism system. These controllers are designed via a quicker and easier method in conjuction with the concept of the hitting condition. Numerical results are provided to compare these controllers and to show that the dynamic behaviour of the proposed controller-motor-mechanism systems are robust with respect to external disturbances.

1. INTRODUCTION

Motion control technologies have been widely used in industrial applications. Due to the fact that good technologies allow for high productivity and produce products of high quality, the study of motion control is a significant topic. The toggle mechanism [1] has many applications, in which a large resistance is overcome with a small driving force, for instance, clutches, rock crushers, truck tailgates, vacuum circuit breakers, punching machines, forging machines, injection modelling machines, etc. The important feature is its ability to produce high-value force at the slider with relatively low torque input. The quick-return mechanism [2] is used for the purpose of giving a slow cutting stroke and a quick-return stroke with a constant angular velocity of the driving crank. There are many types of this kind of mechanism, such as crank-shaper, power-driven saw, drag link, offset slider crank, and so on.

In recent years, there have been many successful applications on fuzzy control, but several difficulties still exist in the fuzzy logical controller (FLC) design. For example: (1) Fuzzy control rules are experience-oriented. Thus, the designer will find it difficult to establish the fuzzy rule bases. (2) Characteristics of the fuzzy control systems cannot be pre-specified. (3) If p is the number of fuzzy sets for input variables, then the complete rule bases are equal to $p \times p$. This will cause the controller rule bases to be too huge to lower the performance of the controlled system. (4) The scaling factors of fuzzy logic controllers are fixed, and cannot be employed for the unknown conditions.

0022-460X/00/280471 + 19 $35.00/0

To overcome the above difficulties (1) and (2) in the FLC design, we adopt the FSMC which uses both s and $\dot{s}$ as the inputs, and apply the sliding mode control techniques to obtain the fuzzy control base. Although the difficulties (1) and (2) are solved by the FSMC, it does not reduce the control rules. In order to solve difficulty (3), we adopt the RLFSMC [3], which combines two input variables of the FSMC as a new one, and the number of fuzzy control rules will be reduced effectively. In the FLC and FSMC, the fixed scaling factors hardly improve the performance of the controller. Thus, the scaling factor tuner (SFT) is designed to tune the scaling factor of the RLFSMC, and to have the best fitness for many unknown conditions.

The organization of this paper is arranged as follows. In section 2, the kinematic and dynamic analyses of the toggle and quick-return mechanisms are briefly discussed. The field-oriented PM synchronous motor is introduced in section 3. The FSMC and the RLFSMC associated with the SFT are designed in sections 4 and 5 respectively. The numerical results are compared for the motor-mechanism systems with the FSMC and RLFSMC. Finally, some conclusions are drawn in section 7.

2. KINEMATIC AND DYNAMIC ANALYSIS OF MECHANISM

2.1. CO-ORDINATE PARTITIONING METHOD

In kinematic analysis, we use the co-ordinate partitioning method [4] to partition the co-ordinate vector as

$$\Psi = [\Psi_1 \ \Psi_2 \cdots \Psi_n]^{\mathrm{T}} = [\mathbf{u}^{\mathrm{T}} \mathbf{v}^{\mathrm{T}}]^{\mathrm{T}}, \tag{1}$$

where $\mathbf{u} = [u_1 \ u_2 \cdots u_m]^{\mathrm{T}}$ and $\mathbf{v} = [v_1 \ v_2 \cdots v_k]^{\mathrm{T}}$ are the m dependent and k independent co-ordinates respectively. The m constraint equations are

$$\Phi = \Phi(\Psi) = \mathbf{0} \tag{2a}$$

or

$$\Phi = \Phi(\mathbf{u}, \mathbf{v}) = \mathbf{0}. \tag{2b}$$

Since the k independent co-ordinates are specified at each instant of time t, equation (2) becomes a set of m equations in m unknowns, which can be solved for the m dependent co-ordinates. If the constraints of equation (2a) are independent, the existence of solution $\mathbf{u}$ for given $\mathbf{v}$ is asserted by the implicit function theory [5]. Differentiating equation (2a) yields the constraint velocity equation

$$\Phi_\Psi \dot{\Psi} = \mathbf{0}, \tag{3}$$

where matrix $\Phi_\Psi = [\partial \Phi / \partial \Psi]$ is the partial derivatives of the constraint equations and is called the constraint Jacobian matrix. Sequentially, equation (3) is rewritten in a partitioned form as

$$\Phi_{\mathbf{u}} \dot{\mathbf{u}} = -\Phi_{\mathbf{v}} \dot{\mathbf{v}}, \tag{4}$$

where $\Phi_{\mathbf{u}}$ and $\Phi_{\mathbf{v}}$ are two submatrices of Φ_Ψ. Since the m constraint equations (2a) are assumed to be independent, then $\Phi_{\mathbf{u}}$ is an $m \times m$ non-singular matrix. Equation (4) may be

solved for $\dot{\mathbf{u}}$, once $\dot{\mathbf{v}}$ is given. Differentiating the constraint velocity equation (3) yields the acceleration equation

$$\Phi_\Psi \ddot{\Psi} = -(\Phi_\Psi \dot{\Psi})_\Psi \dot{\Psi} \equiv \gamma, \tag{5}$$

where $\ddot{\Psi} = [\ddot{\Psi}_1 \ \ddot{\Psi}_2 \cdots \ddot{\Psi}_n]^{\mathrm{T}}$ is a acceleration vector. In the mean time, equation (5) can be written in a partitioned form as

$$\Phi_{\mathbf{u}} \ddot{\mathbf{u}} = -\Phi_{\mathbf{v}} \ddot{\mathbf{v}} - (\Phi_\Psi \dot{\Psi})_\Psi \dot{\Psi}. \tag{6}$$

Since $\Phi_{\mathbf{u}}$ is non-singular, equation (6) can be solved for $\ddot{\mathbf{u}}$, once $\ddot{\mathbf{v}}$ is given. Note that the velocity equation (4) and acceleration equation (6) are two sets of linear algebraic equations in $\dot{\Psi}$ and $\ddot{\Psi}$ respectively.

The Euler–Lagrange equations, accounting for both applied and constraint forces, are

$$\mathbf{M}(\Psi)\ddot{\Psi} + \mathbf{N}(\Psi, \dot{\Psi}) + \Phi_\Psi^{\mathrm{T}} \lambda = \mathbf{B}\mathbf{U}, \tag{7}$$

where $\mathbf{M}$ is the mass matrix, $\mathbf{N}$ is the non-linear vector, λ is the Lagrange multipliers, $\mathbf{B}$ is a constant matrix and $\mathbf{U}$ is the vector of applied forces. We combine equations (5) and (7) to obtain the differential-algebraic equation in the matrix form as

$$\begin{bmatrix} \mathbf{M} & \Phi_\Psi^{\mathrm{T}} \\ \Phi_\Psi & \mathbf{0} \end{bmatrix} \begin{bmatrix} \ddot{\Psi} \\ \lambda \end{bmatrix} = \begin{bmatrix} \mathbf{B}\mathbf{U} - \mathbf{N}(\Psi, \dot{\Psi}) \\ \gamma \end{bmatrix}. \tag{8}$$

The implicit function method will be employed to solve equation (8) by reordering and partitioning. According to the decomposition of Ψ into $\mathbf{u}$ and $\mathbf{v}$, we have

$$\mathbf{M}^{\mathbf{vu}} \ddot{\mathbf{u}} + \mathbf{M}^{\mathbf{vv}} \ddot{\mathbf{v}} + \Phi_{\mathbf{v}}^{\mathrm{T}} \lambda = \mathbf{B}^{\mathbf{v}} \mathbf{U} - \mathbf{N}^{\mathbf{v}}, \qquad \mathbf{M}^{\mathbf{uu}} \ddot{\mathbf{u}} + \mathbf{M}^{\mathbf{uv}} \ddot{\mathbf{v}} + \Phi_{\mathbf{u}}^{\mathbf{T}} \lambda = \mathbf{B}^{\mathbf{u}} \mathbf{U} - \mathbf{N}^{\mathbf{u}}, \tag{9}$$

$$\Phi_{\mathbf{u}} \ddot{\mathbf{u}} + \Phi_{\mathbf{v}} \ddot{\mathbf{v}} = \gamma.$$

Since the coefficient matrix $\Phi_{\mathbf{u}}^{\mathrm{T}}$ of λ in the second of equation (9) is non-singular, this equation could be solved for λ as

$$\lambda = (\Phi_{\mathbf{u}}^{-1})^{\mathbf{T}} [\mathbf{B}^{\mathbf{u}} \mathbf{U} - \mathbf{N}^{\mathbf{u}} - \mathbf{M}^{\mathbf{uv}} \ddot{\mathbf{v}} - \mathbf{M}^{\mathbf{uu}} \ddot{\mathbf{u}}]. \tag{10}$$

Substituting equations (6) and (10) into the first of equation (9), we can obtain

$$\hat{\mathbf{M}}(\mathbf{v})\ddot{\mathbf{v}} + \hat{\mathbf{N}}(\mathbf{v}, \dot{\mathbf{v}}) = \hat{\mathbf{Q}}\mathbf{U}, \tag{11}$$

where

$$\hat{\mathbf{M}} = \mathbf{M}^{\mathbf{vv}} - \mathbf{M}^{\mathbf{vu}} \Phi_{\mathbf{u}}^{-1} \Phi_{\mathbf{v}} - \Phi_{\mathbf{v}}^{\mathrm{T}} (\Phi_{\mathbf{u}}^{-1})^{\mathrm{T}} [\mathbf{M}^{\mathbf{uv}} - \mathbf{M}^{\mathbf{uu}} \Phi_{\mathbf{u}}^{-1} \Phi_{\mathbf{v}}],$$

$$\hat{\mathbf{N}} = [\mathbf{N}^{\mathbf{v}} - \Phi_{\mathbf{v}}^{\mathrm{T}} (\Phi_{\mathbf{u}}^{-1})^{\mathbf{T}} \mathbf{N}^{\mathbf{u}}] + [\mathbf{M}^{\mathbf{vu}} \Phi_{\mathbf{u}}^{-1} - \Phi_{\mathbf{v}}^{\mathrm{T}} (\Phi_{\mathbf{u}}^{-1})^{\mathbf{T}} \mathbf{M}^{\mathbf{uu}} \Phi_{\mathbf{u}}^{-1}] \gamma,$$

$$\hat{\mathbf{Q}} = \mathbf{B}^{\mathbf{v}} - \Phi_{\mathbf{v}}^{\mathrm{T}} (\Phi_{\mathbf{u}}^{-1})^{\mathrm{T}} \mathbf{B}^{\mathbf{u}}.$$

The result is a set of differential equation with only one independent generalized co-ordinate **v**. The system becomes an initial-value problem and can be integrated by using fourth order Runge–Kutta method [6].

2.2. DYNAMIC ANALYSIS OF THE TOGGLE MECHANISM

The matrix element of the differential-algebraic equation (8) can be found in Appendix A. Equations (8) and (A6) may be reordered and partitioned according to the decomposition of $\Psi = [\mathbf{u}^T\ \mathbf{v}^T]^T$. If the constraints are independent, the matrix Φ_ψ has full row rank and there is always at least one non-singular sub-matrix Φ_ψ of rank 3. Gauss–Jordan reduction of the matrix Φ_ψ with double pivoting defines a partitioning of $\Psi = [\mathbf{u}^T\ \mathbf{v}^T]^T$, $\mathbf{u} = [\theta_5\ \theta_3]^T$, $\mathbf{v} = [\theta_2]^T$ such that $\Phi_\mathbf{u}$ is the sub-matrix of Φ_ψ whose columns correspond to elements u of θ, and Φ_v is the sub-matrix of Φ_ψ whose columns correspond to element v of Ψ. The elements of the vectors **u**, **v** and matrices Φ_u, Φ_v, $\mathbf{M}^{uu}$, $\mathbf{M}^{uv}$, $\mathbf{M}^{vu}$ and $\mathbf{M}^{vv}$ of equation (11) are detailed in Appendix B.

2.3. DYNAMIC ANALYSIS OF THE QUICK-RETURN MECHANISM

The differential-algebraic equation [2] of the quick-return mechanism are summarized in the matrix form of equations (8) and (C1), in which the matrices element can be found in Appendix C. Equations (8) and (C1) could be reordered and partitioned according to the decomposition of $\Psi = [\mathbf{u}^T\ \mathbf{v}^T]^T$. The elements of the vectors **u**, **v** and matrices Φ_u, Φ_v, $\mathbf{M}^{uu}$, $\mathbf{M}^{uv}$, $\mathbf{M}^{vu}$ and $\mathbf{M}^{vv}$ are detailed in Appendix D.

3. THE MOTOR-MECHANISM SYSTEMS

The PM synchronous motor drive system [1] can be simplified to a position and speed control system block diagram, as shown in Figure 1, in which

$$\tau_e = K_t i_q^*, \qquad K_t = \tfrac{3}{2} P L_{md} I_{fd} \qquad H_p(s) = \frac{1}{J_m s + B_m}, \tag{12}$$

where τ_e, K_t, i_q^*, P, L_{md}, I_{fd}, J_m and B_m are the electric torque, torque constant, torque current command, number of pole pairs, d-axis mutual inductance, equivalent d-axis magnetizing current, moment of inertial and damping coefficient respectively.

The toggle mechanism driven by a PM synchronous servomotor is shown in Figure 2 while the quick-return mechanism is shown in Figure 3. The PM synchronous motor system drives a geared speed-reducer associated with a gear ratio

$$n = \frac{n_a}{n_b} = \frac{\tau}{\tau_m} = \frac{\omega_r}{\omega} = \frac{\dot\theta_r}{\dot\theta}, \tag{13}$$

where n, n_a and n_b are the gear ratio and gear numbers, and τ_m, ω_r and θ_r are the load torque, rotor speed and rotor angle.

The torque applied to the ball screw can be obtained as

$$\tau = n(\tau_e - J_m\dot\omega_r - B_m\omega_r) = n(K_t i_q^* - nJ_m\ddot\theta - nB_m\dot\theta).$$

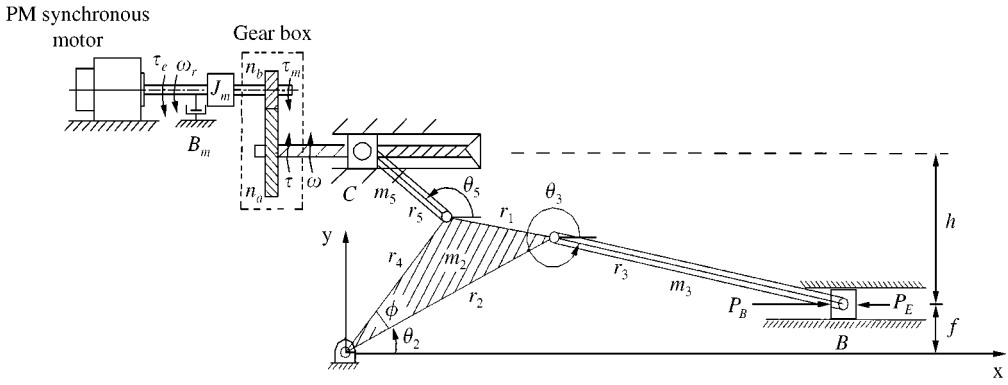

Figure 1. Toggle mechanism driven by a PM synchronous servomotor.

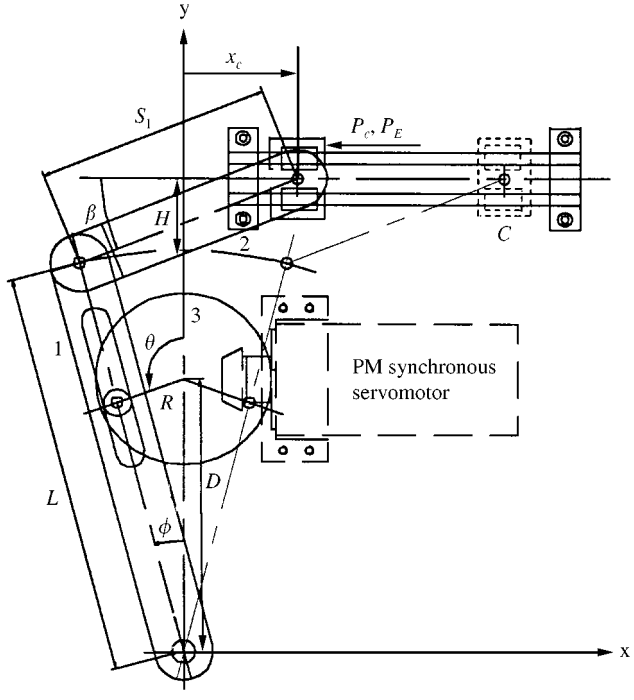

Figure 2. Quick-return mechanism driven by a PM synchronous servomotor.

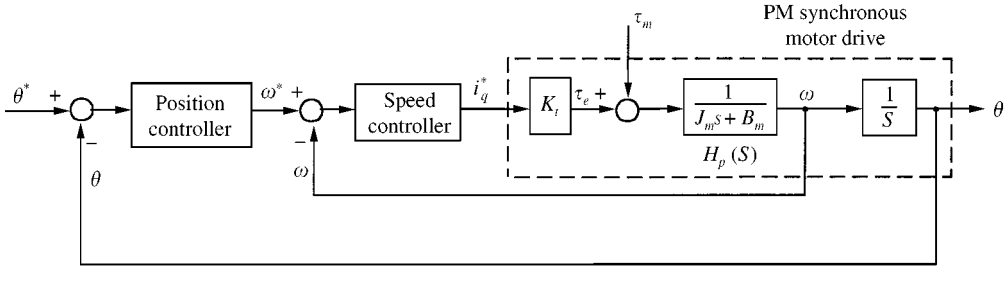

Figure 3. Block diagram of a PM synchronous servomotor drive system.

The screw is a medium that makes the smaller torque τ convert into a larger P_B force acting on the slider B. The conversion relationship is

$$\tau = \frac{P_B L_d}{2\pi n},$$

where L_d is the lead of screw. It should be noted that there is no ball screw in the quick-return mechanism.

4. DESIGN OF THE FSMC

In general, it is hard to obtain the bound of uncertainties and the exact mathematical model in designing a sliding mode control system. Figure 4 is a block diagram of a PM synchronous servomotor drive via a fuzzy sliding mode controller for the toggle mechanism while Figure 5 represents the quick-return mechanism. In the FSMC as shown in Figure 4, the switching function is $s = Ce + \dot{e}$ and e is the error of angle position, and the signals s and $\dot{s}$ are selected as the inputs. In practical implementation, $\dot{s}$ can be approximated by

$$\dot{s}(KT) = \frac{1}{T}[s(KT) - s((K-1)T)], \tag{14}$$

where K is the number of iteration and T is the sampling period [7]. The output of the FSMC is Δu which denotes the change of the controller output. The signals s and $\dot{s}$ must be transferred to their corresponding universes of discourse by multiplying scaling factors GS and GCS, respectively, namely,

$$S = s^* GS, \qquad \dot{S} = \dot{s}^* GCS. \tag{15}$$

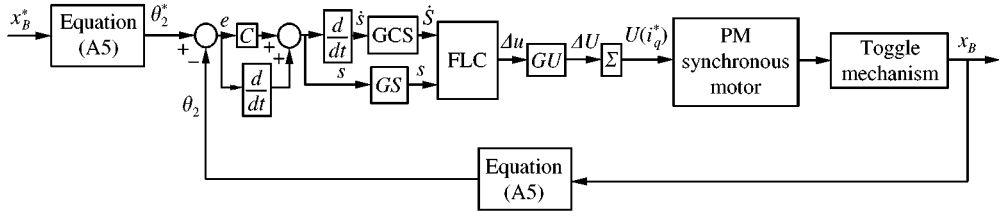

Figure 4. Block diagram of a fuzzy sliding mode controller for the motor-toggle mechanism.

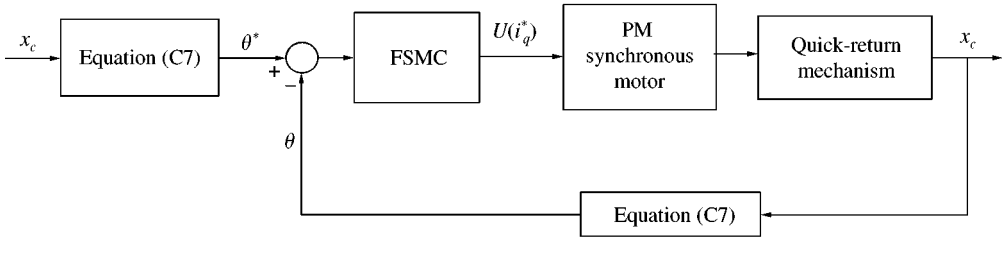

Figure 5. Block diagram of a fuzzy sliding mode controller for the motor-quick-return mechanism.

Since the output Δu of the FSMC is in its corresponding universe of discourse, the Δu could be transferred, by multiplying a scaling factor GU, namely,

$$\Delta U = \Delta u^* GU \tag{16}$$

and the actual input is

$$U(KT + T) = U(KT) + \Delta U(KT + T). \tag{17}$$

It is necessary to quantify the qualitative statements, and the linguistic control rules [8] are defined as follows:

N: Negative,	Z: Zero,	P: Positive,
NH: Negative Huge,	NB: Negative Big,	NM: Negative Medium,
NS: Negative Small,	ZE: Zero,	PS: Positive Small,
PM: Positive Medium,	PB: Positive Big,	PH: Positive Huge.

Thus, the statement of the control rule is: If the S is NB and $\dot{S}$ is NB, then the input Δu to the system is PH.

In order to compare the FSMC and RLFSMC, the membership function of the two mechanisms are chosen as the same, and these fuzzy sets corresponding to S, $\dot{S}$ or Δu are defined in Figure 6. The resulting fuzzy sliding mode control rules are shown in Table 1.

5. DESIGN OF THE RLFSMC

One important problem involved with the design of the FSMC is the complexity of fuzzy controllers, which increases as the number of fuzzy if–then rules increases, and the number of rules increases exponentially as the number of input variables of fuzzy controller increases. If p is the number of fuzzy sets for S and $\dot{S}$, then the complete rule bases are equal to $p \times p$. In order to reduce the number of fuzzy control rules in the FSMC, we adopt the region-wise linear technique to design the FSMC.

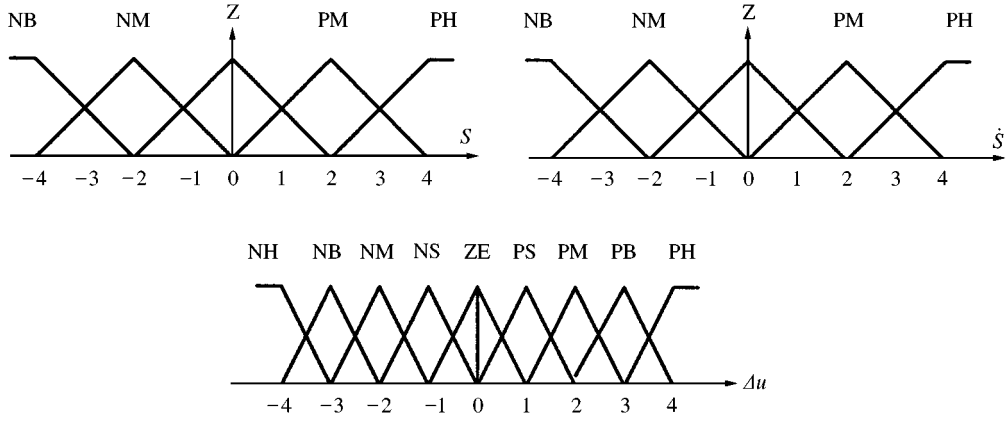

Figure 6. Membership functions of S, $\dot{S}$ and Δu for the toggle and quick-return mechanisms.

From Table 1, we can find the fuzzy control rule bases for the FSMC are symmetric, and the output variable of the controller depends on the negative weight sum of two input variables [9]. Therefore, we defined

$$S^* = S + \dot{S} \tag{18}$$

as the input to the RLFSMC. The block diagram of control are shown in Figures 7 and 8 for the toggle and quick-return mechanisms respectively.

Let the input and output fuzzy variables of the RLFSMC have nine linguist labels which are denoted by PH, PB, PM, PS, ZE, NS, NM, NB, and NH. The relationships between S^*, S and $\dot{S}$ for the toggle and quick-return mechanisms are the same and are listed in Table 2. The rule base for the RLFSMC is shown in Table 3 and has only nine fuzzy if–then rules in its rule base. It is easier than that of the FSMC. The change of control signal for the RLFSMC can be calculated by

$$\Delta U(KT + T) = RLFSMC[S^*(KT + T)]^* GU \tag{19}$$

and the actual input is

$$U(KT + T) = U(KT) + \Delta U(KT + T). \tag{20}$$

The membership function of the RLFSMC variable $S^*$and ΔU for the toggle and quick-return mechanisms is shown in Figure 9.

TABLE 1

The linguistic rules based on the FSMC for the toggle and quick-return mechanisms

		$\dot{S}$				
Δu		NB	NM	Z	PM	PB
S	NB	PH	PB	PM	PS	ZE
	NM	PB	PM	PS	ZE	NS
	Z	PM	PS	ZE	NS	NM
	PM	PS	ZE	NS	NM	NB
	PB	ZE	NS	NM	NB	NH

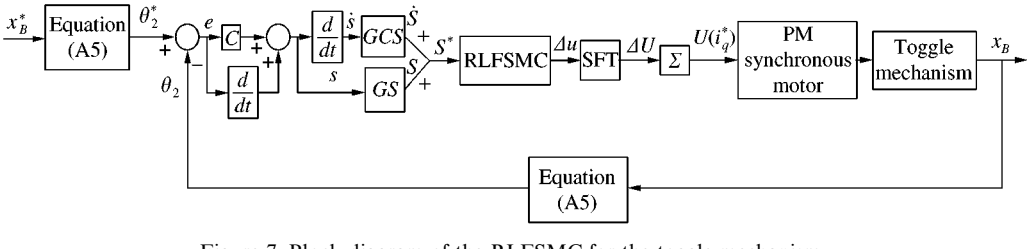

Figure 7. Block diagram of the RLFSMC for the toggle mechanism.

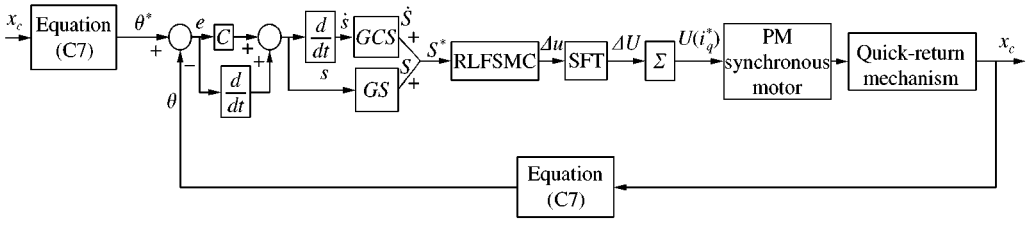

Figure 8. Block diagram of the RLFSMC for the quick-return mechanism.

TABLE 2

The relationships between S, S and $\dot{S}$*

		$\dot{S}$				
	S^*	NB	NM	Z	PM	PB
	NB	NH	NB	NM	NS	ZE
	NM	NB	NM	NS	ZE	PS
S	Z	NM	NS	ZE	PS	PM
	PM	NS	ZE	PS	PM	PB
	PB	ZE	PS	PM	PB	PH

TABLE 3

The rule base for the RLFSMC

S^*	PH	PB	PM	PS	ZE	NS	NM	NB	NH
Δu	NH	NB	NM	NS	ZE	PS	PM	PB	PH

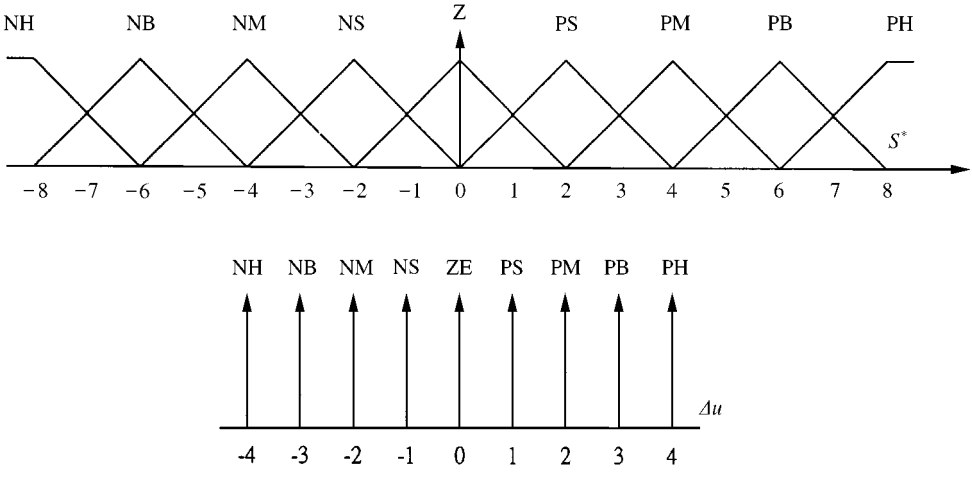

Figure 9. Membership functions of S^* and ΔU of the RLFSMC.

5.1. RLFSMC WITH SCALING FACTOR TUNER

In the fuzzy control system, the scaling factor plays an important role for the system's stability and performance. A large scaling factor for the output may cause the system response with smaller rise time but may result in chattering, while a small scaling factor for the output may cause the rise time of the system to become very long and even make the system unstable.

To achieve the control objective, a scaling factor tuner (SFT) is designed to tune the scaling factor GU. The control signal is determined by the following strategies: (1) When the state of the represented point is near or approaching the sliding surface, a small control signal is required. Hence, we reduce the value of GU to shrink the change of control signal so that the control signal can smoothly converge to this suitable value. (2) When the state of the represented point is far from the sliding surface, we need to enlarge the value of GU so as to make the state approach toward the sliding surface. Therefore, the control signal can rapidly converge to the suitable value [3]. The SFT is given by

$$\text{If } s \geqslant -0{\cdot}02, \qquad GU = a^*|e|^{\kappa}, \tag{21a}$$

$$\text{If } s < -0{\cdot}02, \qquad GU = b^*|e|^{\sigma}, \tag{21b}$$

where a, b, κ, and σ are the constants, and e is the error of the actual and desired trajectories.

6. NUMERICAL SIMULATION

In order to compare the FSMC with RLFSMC, the system parameters, membership function of the FSMC and RLFSMC, the coefficient of the hyperplane and external disturbances are chosen to be the same. The switching function $s = Ce + \dot{e}$ with $C = 6$ is taken in the numerical simulations.

The parameters of the motor system [1] are

$$K_t = 0{\cdot}6732 \text{ N m/A},$$
$$\bar{J}_m = 1{\cdot}32 \times 10^{-3} \text{ N m s}^2 = 0{\cdot}066 \text{ N m s rad/V},$$
$$\bar{B}_m = 5{\cdot}78 \times 10^{-3} \text{ N m s/rad} = 0{\cdot}289 \text{ N m/V}.$$

In order to compare the performance of the two controllers clearly, we define the following performance indices J_1 [10] and J_2 [11]:

$$J_1 = \sum_{K=1}^{600} |s(KT)|, \qquad J_2 = \sum_{K=1}^{600} |u(KT)|, \tag{22a,b}$$

where T equals 0·02.

6.1. THE TOGGLE MECHANISM

The control objective of the toggle mechanism is to regulate the position of the slider B from the left end to the right one. The initial position of x_B is 0·1016 m while the desired position of x_B is 0·1416 m.

The parameters [1] of the toggle mechanism are chosen as follows:

$$m_2 = 0{\cdot}98 \text{ kg}, \quad m_3 = 0{\cdot}91 \text{ kg}, \quad m_5 = 0{\cdot}3 \text{ kg}, \quad m_B = 1{\cdot}46 \text{ kg},$$

$$m_C = 1{\cdot}85 \text{ kg}, \quad r_1 = 0{\cdot}07 \text{ m}, \quad r_2 = 0{\cdot}145 \text{ m}, \quad r_3 = 0{\cdot}19 \text{ m},$$

$$r_4 = 0{\cdot}1 \text{ m}, \quad r_5 = 0{\cdot}06 \text{ m}, \quad f = 0{\cdot}025 \text{ m}, \quad h = 0{\cdot}08 \text{ m},$$

$$L_d = 0{\cdot}005 \text{ m}, \quad \mu = 0{\cdot}1, \quad n_r = 1.$$

6.1.1. *Simulation of the FSMC*

Now, the scaling factors of the FSMC are determined by observing the simulation results to minimize the hitting time to the sliding surface. Thus, we choose the scaling factors of the FSMC as

$$\text{If } s \geqslant -0{\cdot}02,\ GS = 80,\ GCS = 1{\cdot}2 \text{ and } GU = 8{\cdot}12, \tag{23a}$$

$$\text{If } s < -0{\cdot}02,\ GS = 2{\cdot}65,\ GCS = 13{\cdot}2 \text{ and } GU = 4{\cdot}4. \tag{23b}$$

6.1.2. *Simulation of the RLFSMC*

The scaling factors and all parameters are selected as

$$\text{If } s \geqslant -0{\cdot}02,\ GS = 80,\ GCS = 1{\cdot}2,\ a = 10{\cdot}12 \text{ and } \kappa = 0{\cdot}9, \tag{24a}$$

$$\text{If } s < -0{\cdot}02,\ GS = 2{\cdot}65,\ GCS = 13{\cdot}2,\ b = 1{\cdot}17 \text{ and } \sigma = 0{\cdot}9. \tag{24b}$$

The compared numerical results of the FSMC and RLFSMC applied to the motor-toggle mechanism are given in Figures 10(a)–(d) and 11(a)–(d) with $P_E = 0$ and 50 N, respectively. The trajectories of slider B shown in Figure 10(a) and the phase plane of the angle position shown in Figure 10(b) are almost the same for the FSMC and RLFSMC. However, the performance indices J_1 and J_2, shown in Figures 10(c) and 10(d), respectively, indicate that the RLFSMC is better than the FSMC.

6.2. THE QUICK-RETURN MECHANISM

In the numerical simulations, the parameters [2] of the quick-return mechanism are chosen as follows:

$$m_1 = 1{\cdot}082 \text{ kg}, \quad m_2 = 0{\cdot}82 \text{ kg}, \quad m_3 = 1{\cdot}1 \text{ kg}, \quad \mathrm{m_c} = 1{\cdot}84 \text{ kg},$$

$$D = 0{\cdot}19 \text{ m}, \quad \mathrm{Q} = 0{\cdot}1595 \text{ m}, \quad L = 0{\cdot}28 \text{ m}, \quad H = 0{\cdot}05 \text{ m},$$

$$r = 0{\cdot}048 \text{ m}, \quad \mu = 0{\cdot}1, \quad n_r = 0{\cdot}5, \quad g = 9{\cdot}8 \text{ m/s}^2.$$

It is clear that the mechanism system has one degree of freedom; the input angle θ will correspond to one and only one output position at slider C. Two cases are addressed in the fuzzy sliding mode control and region-wise linear fuzzy sliding mode control. In all the simulations, the control objective is to regulate the position of the slider C from the left end

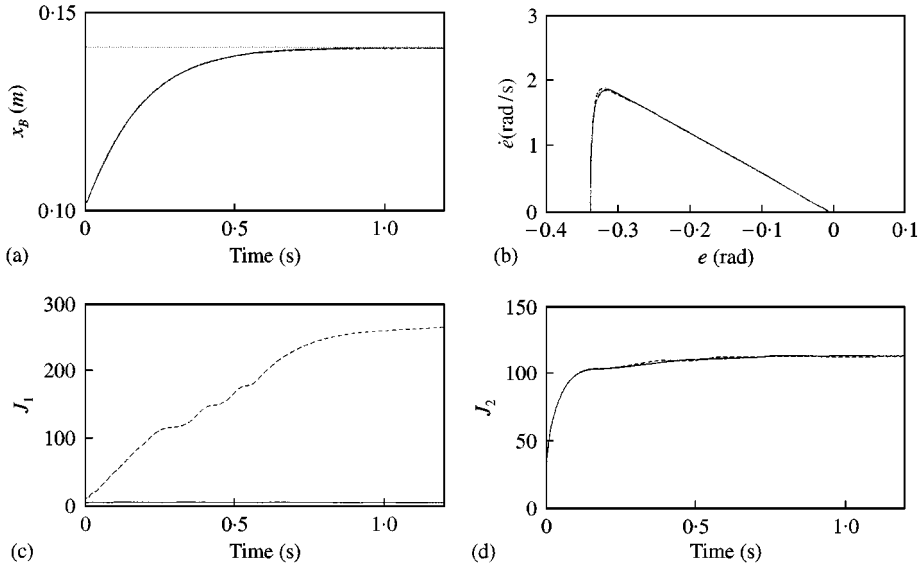

Figure 10. Position regulation of the motor-toggle mechanism via the FSMC and RLFSMC without external disturbance. (a) Slider position x_B. (b) Phase plane of the angle position. (c) Performance index J_1. (d) Performance index J_2 (---: the FSMC; ——: the RLFSMC).

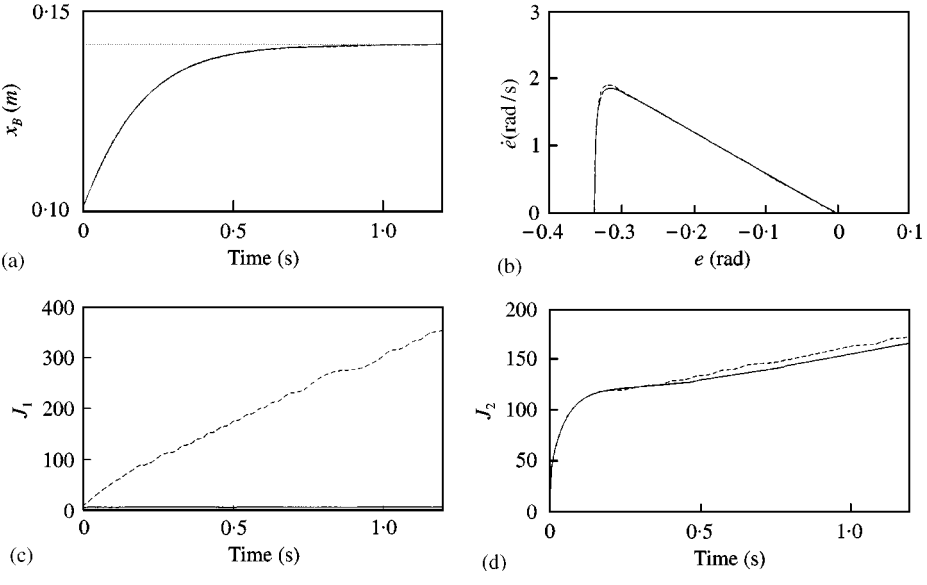

Figure 11. Position regulation of the motor-toggle mechanism via the FSMC and RLFSMC with external disturbance $P_E = 50$ N. (a) Slider position x_B. (b) Phase plane of the angle position. (c) Performance index J_1. (d) Performance index J_2 (---: the FSMC; ——: the RLFSMC).

to the right one. The initial position of x_C is 0·08 m while the desired position of x_C is 0·18 m. Substituting the slider positions x_C into equation (C16), the initial and desired angle θ can be obtained. It should be noted that the friction force P_c is considered in the quick-return mechanism.

6.2.1. *Simulation of the FSMC*

We chose the scaling factors of the FSMC as

$$\text{If } s \geqslant -0{\cdot}02,\ GS = 80,\ GCS = 1{\cdot}2 \text{ and } GU = 8{\cdot}12, \tag{25a}$$

$$\text{If } s < -0{\cdot}02,\ GS = 2{\cdot}65,\ GCS = 13{\cdot}2 \text{ and } GU = 4{\cdot}4. \tag{25b}$$

In the simulation of the FSMC applied to the quick-return mechanism, the system becomes unstable by using the same membership of the toggle mechanism. It is shown that the FSMC is not suitable for all the mechanisms with the same membership. The Δu is determined by the shape of membership and the actual input U is calculated by equation (17). It is known that the increasing control input as shown in equation (17) may not satisfy the reaching condition $s\dot{s} < 0$ [12] and cause the system to be unstable.

6.2.2. *Simulation of the RLFSMC*

The scaling factors and all parameters are selected as

$$\text{If } s \geqslant -0{\cdot}02, \quad GS = 80, \quad GCS = 1{\cdot}2, \quad a = 0{\cdot}25 \text{ and } \kappa = 0{\cdot}4, \tag{26a}$$

$$\text{If } s < -0{\cdot}02, \quad GS = 2{\cdot}65, \quad GCS = 13{\cdot}2, \quad b = 0{\cdot}807 \text{ and } \sigma = 0{\cdot}7. \tag{26b}$$

The simulation results of the RLFSMC applied to the quick-return mechanism are given in Figures 12(a)–(d) for the external disturbances $P_E = 0$ (dash lines) and 5 N (solid lines). It is seen that the motor mechanism via the RLFSMC is successfully controlled and is robust with respect to the external disturbances. The performance index J_2 of the system considering the external disturbance is larger than that without the disturbance.

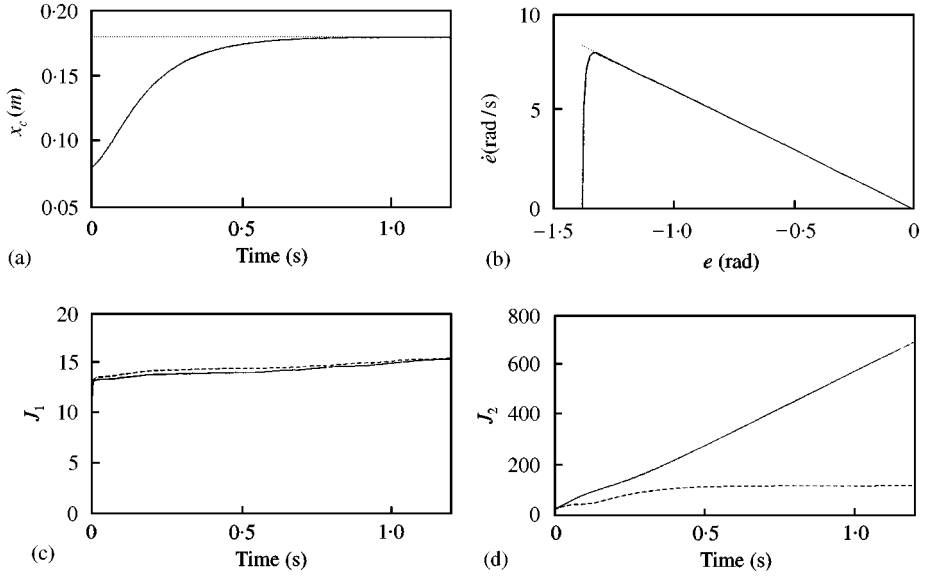

Figure 12. Position regulation of the motor-quick-return mechanism via the RLFSMC. (a) Slider position x_C. (b) Phase plane of the angle position. (c) Performance index J_1. (d) Performance index J_2 (---: $P_E = 0$; ——: $P_E = 5$ N).

7. CONCLUSIONS

This paper successfully proposes the FSMC and RLFSMC to the position control of the toggle and quick-return mechanisms driven by the PM synchronous motor. The numerical results of the RLFSMC are similar to those via the FSMC for the toggle mechanism, and the performance indices of the RLFSMC are better than the FSMC. However, the FSMC fails in the simulations of the quick-return mechanism. This is due to the fact that the FSMC with a fixed scaling factor is only suited for some conditions. The RLFSMC can fit more unknown conditions by using the SFT to tune the scaling factors in the motor-mechanism systems. Besides, the RLFSMC has only nine fuzzy if–then rules in its rule base. We can achieve almost the real-time control in the implementations.

From the designs of controllers and the numerical results, several conclusions can be drawn:

1. By using the technique of the FSMC, the designer can easily establish the fuzzy control rule bases. By using the technique of the RLFSMC, the complexity of the fuzzy controller and the computational time can be reduced.
2. The RLFSMC is suited for more unknown conditions by using a scaling factor tuner to tune its factors. Thus, it is better than the FSMC with a fixed scaling factor.
3. Robust performance of the controller-motor-mechanism system can be achieved by the FSMC and RLFSMC with respect to external disturbances.

REFERENCES

1. R. F. FUNG, F. J. LIN and Y. C. WANG 1997 *IEE Proceedings Control Theory Applications* **144**, 393–402. Sliding mode and fuzzy control of toggle mechanism using PM synchronous servomotor drive.
2. R. F. FUNG and Y. C. WANG 1997 *The Japan Society of Mechanical Engineers, Series C* **40**, 454–641. Constant speed control of the quick return mechanism driven by a DC motor.
3. C. C. KUNG and W. C. LAI 1999 *Conference* on *Automatic Control, Taiwan*, 97–105. Region-wise fuzzy sliding mode controller design.
4. E. N. PARVIZ 1988 *Computer-Aided Analysis of Mechanical System*. Englewood Cliffs, NJ: Prentice-Hall.
5. R. F. FUNG and K. W. CHEN 1998 *Journal of Sound and Vibration* **212**, 721–742. Vibration suppression motion control of a non-linearly coupled flexible quick-return mechanism driven by a PM synchronous servo motor.
6. R. F. FUNG, C. C. HWANG, C. S. HUANG and W. P. CHEN 1997 *Computers & Structures* **63**, 91–99. Inverse dynamics of a toggle mechanism.
7. R. F. FUNG, K. W. CHEN and J. Y. YEN 1999 *International Journal of Mechanical Science* **41**, 337–355. Fuzzy sliding mode controlled slider-crank mechanism using PM synchronous servo motor drive.
8. Y. F. LI and C. C. LAU 1989 *IEEE Control Systems Magazine* 65–71. Development of fuzzy algorithms for servo system.
9. J. S. TAUR and C. W. TAO 1997 *IEEE Transactions on System, Man, and Cybernetics—Part B: Cybernetics* **27**, 526–532. Design and analysis of region-wise linear fuzzy controller.
10. C. L. CHEN and M. H. CHANG 1998 *Fuzzy Sets and Systems* **93**, 37–48. Optimal design of fuzzy sliding-mode control: a comparative study.
11. K. D. YOUNG and Ü. ÖZGÜNER 1997 *Automatica* **33**, 1313–1323. Sliding-mode design for robust linear optimal control.
12. V. I. UTKIN 1992 *Sliding Modes in Control and Optimization*. New York: Springer-Verlag.

APPENDIX A: KINEMATIC AND DYNAMIC ANALYSIS OF THE TOGGLE MECHANISM

The motor-mechanism coupled system is shown in Figure 2, where links 2, 3 and 5 comprise a toggle mechanism with an offset f. The h is the height between two horizontal

guides where sliders B and C move along. A PM synchronous motor, gearbox and ball screw are used to transfer the power. If the external force exerts on the slider C, links 5, 2 and 3 are then driven and the output force at slider B rises.

From the geometry of Figure 2, two relational equations in the y direction can be found as

$$r_2 \sin\theta_2 = f + r_3 \sin(2\pi - \theta_3), \tag{A1}$$

$$r_5 \sin(\pi - \theta_5) + r_4 \sin(\theta_2 + \phi) = h + f. \tag{A2}$$

The position vector of the slider B can be expressed in the exponential form:

$$h_B = r_2 e^{i\theta_2} + r_3 e^{i\theta_3}. \tag{A3}$$

Using equation (A1) and expanding equation (A2) in terms of trigonometry, we have

$$x_B = r_2 \cos\theta_2 + [r_3^2 - (f - r_2 \sin\theta_2)^2]^{1/2}, \tag{A4}$$

$$\theta_2 = \sin^{-1}\left[\frac{x_B^2 + r_2^2 + f^2 - r_3^2}{2r_2\sqrt{x_B^2 + f^2}}\right] - \sin^{-1}\sqrt{\frac{x_B}{x_B^2 + f^2}}, \tag{A5}$$

where x_B is the real part of h_B. If θ_2 is given, the position of the slider B can be determined from equation (A4). While x_B is given, the angle θ_2 of link 2 can be determined from equation (A5). It should be noted that the relationship between x_B and θ_2 is one-to-one.

Fung *et al.* [6] have exploited the holomonic constraint equation

$$\Phi(\Psi) = \begin{bmatrix} r_3 \sin\theta_3 + r_2 \sin\theta_2 - f \\ r_5 \sin\theta_5 + r_4 \sin(\theta_2 + \phi) - h - f \end{bmatrix} = 0, \tag{A6}$$

where $\Psi = [\theta_5\ \theta_3\ \theta_2]^T$ is the vector of generalized co-ordinates. Hamilton's principle and Lagrange multiplier were used to derive the differential-algebraic equation for the toggle mechanism [6]. The Euler–Lagrange equation of motion, accounting for both applied and constraint forces, is the same with equation (7) associated with the coefficients

$$\mathbf{M} = \begin{bmatrix} A & 0 & E \\ 0 & B & H \\ E & H & C \end{bmatrix},$$

$$\mathbf{N} = \begin{bmatrix} I & 0 & J \\ 0 & K & O \\ P & Q & R \end{bmatrix} \begin{Bmatrix} \dot\theta_5^2 \\ \dot\theta_3^2 \\ \dot\theta_2^2 \end{Bmatrix} + \begin{bmatrix} T & 0 & V \\ 0 & 0 & 0 \\ W & 0 & Y \end{bmatrix} \begin{Bmatrix} \dot\theta_5 \\ \dot\theta_3 \\ \dot\theta_2 \end{Bmatrix} - \begin{bmatrix} 0 \\ (P_B - P_E) r_3 \sin\theta_3 \\ (P_B - P_E) r_2 \sin(\theta_2 + \phi) \end{bmatrix},$$

$$\mathbf{B} = \begin{bmatrix} K_t Z r_5 \sin\theta_5 \\ 0 \\ K_t Z r_4 \sin\theta_2 \end{bmatrix}, \qquad \mathbf{U} = [i_q^*]$$

in which P_B is the applied force acting on the slider B, P_E is the external disturbance force and

$$A = -\frac{1}{2}\left(\frac{2}{3}m_5 + 2m_C \sin^2\theta_5\right)r_5^2 - J_m Z^2 r_5^2 \sin^2\theta_5, \qquad B = -\frac{1}{2}\left\{\left(\frac{2}{3}m_3 + 2m_B \sin^2\theta_3\right)r_3^2\right\},$$

$$C = -\frac{1}{2}\left\{\frac{m_2 r_2^2 r_4^2}{r_1^2}\sin^2\phi + 2(m_3 + m_B)r_2^2 \sin^2\theta_2 + 2(m_5 + m_C + J_m Z^2)r_4^2 \sin^2(\theta_2 + \phi)\right\},$$

$$E = -\tfrac{1}{2}\{(2m_C + m_5)r_4 r_5 \sin(\theta_2 + \phi)\sin\theta_5\} - J_m Z^2 r_5 \sin\theta_5 r_4 \sin(\theta_2 + \phi),$$

$$H = -\tfrac{1}{2}\{(2m_B + m_3)r_2 r_3 \sin\theta_2 \sin\theta_3\}, \; I = -\tfrac{1}{2}\{2m_C r_5^2 \sin\theta_5 \cos\theta_5\} - J_m Z^2 r_5^2 \sin\theta_5 \cos\theta_5,$$

$$J = -\tfrac{1}{2}\{(m_5 + 2m_C)r_4 r_5 \cos(\theta_2 + \phi)\sin\theta_5\} - J_m Z^2 r_5 \sin\theta_5 r_4 \cos(\theta_2 + \phi),$$

$$K = -\tfrac{1}{2}(2m_B r_3^2 \sin\theta_3 \cos\theta_3), \qquad O = -\tfrac{1}{2}\{(m_3 + 2m_B)r_2 r_3 \cos\theta_2 \sin\theta_3\},$$

$$P = -\tfrac{1}{2}\{(m_5 + 2m_C)r_4 r_5 \sin(\theta_2 + \phi)\cos\theta_5\} - J_m Z^2 r_4 r_5 \sin(\theta_2 + \phi)\cos\theta_5,$$

$$Q = -\tfrac{1}{2}\{(m_3 + 2m_B)r_2 r_3 \sin\theta_2 \cos\theta_3\},$$

$$R = -\tfrac{1}{2}\{2(m_3 + m_B)r_2^2 \sin\theta_2 \cos\theta_2 + 2(m_5 + m_C + 1/2\, J_m Z^2)r_4^2 \sin(\theta_2 + \phi)\cos(\theta_2 + \phi)\},$$

$$T = -B_m Z^2 r_5^2 \sin^2\theta_5, \qquad V = -B_m Z^2 r_5 \sin\theta_5 r_4 \sin(\theta_2 + \phi),$$

$$W = -B_m Z^2 r_4 \sin(\theta_2 + \phi) r_5 \sin\theta_5, \qquad Y = -B_m Z^2 r_4^2 \sin^2(\theta_2 + \phi),$$

and $Z = 2\pi n/Ld$, n is the gear ratio and Ld is the lead of screw.

APPENDIX B: MATRICES OF THE DECOUPLED EQUATION OF THE TOGGLE MECHANISM

For the toggle mechanism, we choose

$$\mathbf{v} = [\theta_2], \qquad \mathbf{u} = [\theta_5 \;\; \theta_3]^{\mathrm{T}}, \qquad \Phi_{\mathbf{v}} = \begin{bmatrix} r_2 \cos\theta_2 \\ r_4 \cos(\theta_2 + \phi) \end{bmatrix} \quad \text{and} \quad \Phi_{\mathbf{u}} = \begin{bmatrix} 0 & r_3 \cos\theta_3 \\ r_5 \cos\theta_5 & 0 \end{bmatrix}.$$

The determinant of $\Phi_{\mathbf{u}}$ is $-r_3 r_5 \cos\theta_3 \cos\theta_5$ and is full stroke; there is no such θ_3 and θ_5 that make the determinant of $\Phi_{\mathbf{u}} = 0$. Therefore this partitioning of $\Psi = [\mathbf{u}^{\mathrm{T}} \; \mathbf{v}^{\mathrm{T}}]^{\mathrm{T}}$ is suitable. The element of vector and matrices of equation (10) are

$$\mathbf{M}^{\mathbf{uu}} = \begin{bmatrix} A & 0 \\ 0 & B \end{bmatrix}, \qquad \mathbf{M}^{\mathbf{uv}} = \begin{bmatrix} E \\ H \end{bmatrix}, \qquad \mathbf{M}^{\mathbf{vu}} = [E \;\; H], \qquad \mathbf{M}^{\mathbf{vv}} = [C],$$

$$\mathbf{N^u} = \begin{bmatrix} I & 0 & J \\ 0 & K & O \end{bmatrix} \begin{Bmatrix} \dot{\theta}_5^2 \\ \dot{\theta}_3^2 \\ \dot{\theta}_2^2 \end{Bmatrix} + \begin{bmatrix} T & 0 & V \\ 0 & 0 & 0 \end{bmatrix} \begin{Bmatrix} \dot{\theta}_5 \\ \dot{\theta}_3 \\ \dot{\theta}_2 \end{Bmatrix} + \begin{bmatrix} 0 \\ (P_B - P_E) r_3 \sin\theta_3 \end{bmatrix},$$

$$\mathbf{N^v} = [P \quad Q \quad R] \begin{Bmatrix} \dot{\theta}_5^2 \\ \dot{\theta}_3^2 \\ \dot{\theta}_2^2 \end{Bmatrix} + [W \quad 0 \quad Y] \begin{Bmatrix} \dot{\theta}_5 \\ \dot{\theta}_3 \\ \dot{\theta}_2 \end{Bmatrix} + [(P_B - P_E) r_2 \sin(\theta_2 + \phi)],$$

$$\mathbf{B^u} = \begin{bmatrix} K_t Z r_5 \sin\theta_5 \\ 0 \end{bmatrix}, \qquad \mathbf{B^v} = [K_t Z r_4 \sin\theta_2],$$

where the entries (e.g., A, B, C, ...) are the same as in Appendix A.

APPENDIX C: KINEMATIC AND DYNAMIC ANALYSIS OF THE QUICK-RETURN MECHANISM

From the geometry of the quick-return mechanism shown in Figure 3, we obtain the following relational equations:

$$\tan\phi = \frac{R\sin\theta}{D + R\cos\theta}, \qquad S_1 \sin\beta - H = L(1 - \cos\phi). \tag{C1, C2}$$

The position vector of the slider C can be expressed in the form

$$x_C = S_1 \cos\beta - L\sin\phi. \tag{C3}$$

Substituting equation (C2) into equation (C3) yields

$$x_C = \{S_1^2 - [L(1 - \cos\phi) + H]^2\}^{1/2} - L\sin\phi, \tag{C4}$$

where

$$\phi = \sin^{-1}\left[\frac{S_1^2 - x^2 - 2L^2 - H^2 - 2LH}{2L(x^2 + (L + H)^2)^{1/2}}\right] + \phi', \tag{C5}$$

$$\phi' = \sin^{-1}\left[\frac{L + H}{(x^2 + (L + H)^2)^{1/2}}\right].$$

Rewriting equation (C2), we can obtain

$$\theta = \sin^{-1}\left(\frac{D}{R}\sin\phi\right) + \phi. \tag{C6}$$

Substituting equation (C5) into equation (C6), we have

$$\theta = \sin^{-1}\left\{\frac{D}{R}\sin\left\{\sin^{-1}\left[\frac{S_1^2 - x^2 - 2L^2 - H^2 - 2LH}{2L(x^2 + (L+H)^2)^{1/2}}\right] + \phi'\right\}\right\}$$

$$+ \sin^{-1}\left[\frac{S_1^2 - x^2 - 2L^2 - H^2 - 2LH}{2L(x^2 + (L+H)^2)^{1/2}}\right] + \phi'. \tag{C7}$$

The holomonic constraint equations of the quick-return mechanism is

$$\Phi(\Psi) = \begin{bmatrix} \sin\phi\,(D + R\cos\theta) - R\sin\theta\cos\phi \\ S_1\sin\beta - L(1-\cos\phi) - \mathrm{H} \end{bmatrix} = 0, \tag{C8}$$

where $\Psi = [\phi\ \beta\ \theta]^{\mathrm{T}}$ is the vector of generalized co-ordinates.

The Euler–Lagrange equation of motion [4], accounting for both applied and constraint forces, is the same as equation (8) associated with the coefficients

$$\mathbf{M} = \begin{bmatrix} A1 & G1 & 0 \\ H1 & B1 & 0 \\ 0 & 0 & CC \end{bmatrix}, \qquad \mathbf{N} = \begin{bmatrix} P1 & T1 & 0 \\ Y1 & R1 & 0 \\ 0 & 0 & 0 \end{bmatrix}\begin{Bmatrix} \dot\phi^2 \\ \dot\beta^2 \\ \dot\theta^2 \end{Bmatrix} + \begin{bmatrix} -(P_C + P_E)L\cos\phi \\ -(P_C + P_E)S_1\sin\beta \\ n^2 B_m\dot\theta \end{bmatrix},$$

$$\mathbf{B} = \begin{bmatrix} 0 \\ 0 \\ -nK_t \end{bmatrix}, \qquad \mathbf{U} = [i_q^*]$$

in which P_E is the external disturbance force, and P_c is the friction force:

$$P_C = \mu m_C g\,\mathrm{sgn}\,(\dot x_C), \qquad \mathrm{sgn}\,(\dot x_C) = \begin{cases} 1 & \text{if } \dot x_C > 0, \\ -1 & \text{if } \dot x_C < 0 \end{cases}$$

and $\dot x_C$ is velocity of the slider C; μ, g are the friction coefficient and gravity acceleration, respectively,

$$A1 = -\frac{1}{3}m_1L^2 - (m_2 + m_C)L^2\cos^2\phi, \qquad G1 = -\left(\frac{1}{2}m_2 + m_C\right)S_1L\sin\beta\cos\phi,$$

$$H1 = -\left(\frac{1}{2}m_2 + m_C\right)S_1L\sin\beta\cos\phi, \qquad B1 = -\left(\frac{1}{3}m_2 + m_C\sin^2\beta\right)S_1^2,$$

$$CC = -\frac{1}{3}m_3R^2 - n^2J_m, \qquad P1 = (m_2 + m_C)L^2\cos\phi\sin\phi,$$

$$T1 = -\left(\frac{1}{2}m_2 + m_C\right)S_1L\cos\beta\cos\phi, \qquad Y1 = \left(\frac{1}{2}m_2 + m_C\right)S_1L\sin\beta\sin\phi,$$

$$R1 = -m_CS_1^2\sin\beta\cos\beta.$$

APPENDIX D: MATRICES OF THE DECOUPLED EQUATION OF THE QUICK-RETURN MECHANISM

We chose $\mathbf{v} = [\theta]$, then $\mathbf{u} = [\phi, \beta]$, and

$$\Phi_{\mathbf{v}} = \begin{bmatrix} -R\sin\phi\sin\theta - \mathrm{R}\cos\theta\cos\phi \\ 0 \end{bmatrix},$$

$$\Phi_{\mathbf{u}} = \begin{bmatrix} \cos\phi(D + R\cos\theta) + R\sin\theta\sin\phi & 0 \\ -L\sin\phi & S_1\cos\beta \end{bmatrix}.$$

The determinant of $\Phi_{\mathbf{u}}$ is $S_1\cos\beta\cos\phi(D + R\cos\theta) + RS_1\cos\beta\sin\theta\sin\phi$ and is non-singular. Since there are no ϕ and β in the analyzed mechanism that makes the determinant of $\Phi_{\mathbf{u}} = 0$, this partitioning of $\Psi = [\mathbf{u}^{\mathrm{T}}, \mathbf{v}^{\mathrm{T}}]^{\mathrm{T}}$ is suitable. The submatrices of equation (10) are

$$\mathbf{M}^{\mathbf{uu}} = \begin{bmatrix} A1 & G1 \\ H1 & B1 \end{bmatrix}, \qquad \mathbf{M}^{\mathbf{uv}} = [0], \qquad \mathbf{M}^{\mathbf{vu}} = [0], \qquad \mathbf{M}^{\mathbf{vv}} = [CC],$$

$$\mathbf{N}^{\mathbf{u}} = \begin{bmatrix} P1 & T1 & 0 \\ Y1 & R1 & 0 \end{bmatrix} \begin{Bmatrix} \dot{\phi}^2 \\ \dot{\beta}^2 \\ \dot{\theta}^2 \end{Bmatrix} + \begin{bmatrix} -(P_C + P_E)L\cos\phi \\ -(P_C + P_E)S_1\sin\beta \end{bmatrix}, \qquad \mathbf{N}^{\mathbf{v}} = [n^2 B_m \theta],$$

$$\mathbf{B}^{\mathbf{u}} = [0], \qquad \mathbf{B}^{\mathbf{v}} = [-nK_t],$$

where the entries (e.g., $C1$, $D1$, $CC, \ldots$) are the same as in Appendix C.